

ALMA observations require slower Core Accretion runaway growth

S. Nayakshin¹, G. Dipierro¹ and J. Szulágyi²

¹ Department of Physics and Astronomy, University of Leicester, University Road, LE1 7RH Leicester, United Kingdom

² Center for Theoretical Astrophysics and Cosmology, Institute for Computational Science, University of Zürich, Winterthurerstrasse 190, CH-805 Switzerland

Accepted XXX. Received YYY; in original form ZZZ

ABSTRACT

Thanks to recent high resolution ALMA observations, there is an accumulating evidence for presence of giant planets with masses from $\sim 0.01 M_{\text{J}}$ to a few M_{J} with separations up to 100 AU in the annular structures observed in young protoplanetary discs. We point out that these observations set unique “live” constraints on the process of gas accretion onto sub-Jovian planets that were not previously available. Accordingly, we use a population synthesis approach in a new way: we build time-resolved models and compare the properties of the synthetic planets with the ALMA data at the same age. Applying the widely used gas accretion formulae leads to a deficit of sub-Jovian planets and an over-abundance of a few Jupiter mass planets compared to observations. We find that gas accretion rate onto planets needs to be suppressed by about an order of magnitude to match the observed planet mass function. This slower gas giant growth predicts that the planet mass should correlate positively with the age of the protoplanetary disc, albeit with a large scatter. This effect is not clearly present in the ALMA data but may be confirmed in the near future with more observations.

Key words: planets and satellites: protoplanetary discs – planets and satellites: gaseous planets – planets and satellites: formation

1 INTRODUCTION

In the Core Accretion paradigm, a solid core grows by accretion of solids (Safronov 1972; Pollack et al. 1996). When the core mass reaches a critical value of $M_{\text{cr}} \sim 10 - 20 M_{\oplus}$, a gas envelope collapses onto the core, fuelling a phase of rapid gas accretion (Mizuno et al. 1978; Ikoma et al. 2000), during which the planet accretion rate is believed to be limited only by the rate at which the disc supplies it with gas. Detailed isothermal simulations showed that the planet may grow from the mass of $\sim 0.1 M_{\text{J}}$ to $\sim (1 - 3) M_{\text{J}}$ in a matter of less than ten thousand years (Bate et al. 2003; D’Angelo et al. 2003). In contrast, dispersal of protoplanetary discs takes ~ 3 Myr (Haisch et al. 2001). A planet is hence destined to become a massive gas giant if it enters the runaway accretion growth phase while the disc is still present.

This runaway gas accretion scenario produces a *valley in the planet mass function* from $M_{\text{p}} \sim 0.1 M_{\text{J}}$ to $M_{\text{p}} \sim 1 M_{\text{J}}$ or more (Ida & Lin 2004a; Mordasini et al. 2009). Early exoplanet observations seemed to confirm this (e.g., see the red histogram in fig. 12 in Mayor et al. 2011). However, a number of new observational and theoretical arguments suggest that gas accretion onto planets is significantly less efficient than hitherto believed. Non-isothermal multi-dimensional simu-

lations suggest that atmospheric circulation and inefficient radiative cooling may reduce accretion rates significantly (Ayliffe & Bate 2009b,a; Ormel et al. 2015; Szulágyi et al. 2016; Szulágyi & Mordasini 2017; Szulágyi 2017; Cimerman et al. 2017; Lambrechts & Lega 2017). This may explain why super-Earth planets with very modest gaseous atmospheres are abundant at separations of ~ 0.1 AU (Lee et al. 2014).

Additionally, the classical positive correlation of gas giants with host star metallicity (Fischer & Valenti 2005), dominated by $\sim 1 M_{\text{J}}$ planets, was found to disappear at higher masses (Santos et al. 2017). The exact mass scale at which the switch in the metallicity correlations takes place is currently debated but is somewhere between $2 - 10 M_{\text{J}}$ (Schlaufman 2018; Adibekyan 2019; Maldonado et al. 2019; Goda & Matsuo 2019). The trend is continuous into the brown dwarf regime (e.g., Troup et al. 2016), and suggests that at least a fraction of the most massive planets forms “as stars” – by disc fragmentation. This also suggests that gas accretion onto $\gtrsim 1 M_{\text{J}}$ mass planets is inefficient as otherwise the positive host metallicity correlation of low mass “seed” giants would be passed on to higher mass planets, and even strengthened (Mordasini et al. 2012a).

Additional support for these ideas comes from the microlensing surveys sensitive to planets with separations of

arXiv:1905.13104v1 [astro-ph.EP] 30 May 2019

a few AU (Suzuki et al. 2016). The mass function of microlensing planets contains too many planets in the mass range $\sim [0.1 - 0.3]M_J$ compared with the runaway accretion scenario (Suzuki et al. 2018). The models were shown to fare better if gas accretion rate onto sub-Jupiter mass planets that open deep gaps in the disc and isolate themselves from the gas supply is reduced. In this scenario, $M_p \gtrsim 1M_J$ may preferentially form by gravitational instability (Suzuki et al. 2018).

ALMA observations of annular structures (rings and gaps) in the dust emission of young protoplanetary discs at $\sim 10 - 100$ AU separations have been interpreted as signs of gas giant planets by many authors (ALMA Partnership et al. 2015; Dipierro et al. 2015; Dong et al. 2018; Long et al. 2018; Andrews et al. 2018). While other interpretations exist (see Discussion), it is important to ask what these candidate planets may mean for planet formation theories. Lodato et al. (2019) (L19 hereafter) considered evolutionary paths of these candidate planets, starting from their observed parameters, and found that they evolve into massive gas giants quickly. We ask a complementary question: *how did the candidate planets evolve to be what they are now?* These $\sim 1 - 10$ Million years old gaseous discs have not yet been dispersed and should fuel planetary growth, giving us the first ever time-resolved observational probe of runaway gas accretion. Furthermore, at large separations the runaway accretion should start at lower core masses (Piso et al. 2015) and terminate at larger masses ($\sim [3 - 10]M_J$, because disc gap-opening is harder), producing a very wide valley from $\sim 0.1M_J$ to $\sim 3M_J$, and an excess of $M_p \sim 10M_J$ planets.

2 THE DATA

Table A shows the masses, separation and ages of the ALMA candidate planets that we use here. Our two major data sources are Long et al. (2018) and the DSHARP (Andrews et al. 2018; Huang et al. 2018) survey. The former lists dust gap widths W , separations, a , stellar masses, M_* , and other relevant information. Following Lodato et al. (2019), we assume that the gap width scales with the planet Hill radius. Most of the hydrodynamical simulations **to date** have shown that W corresponds to the range $(4.5 - 7)R_H$, where $R_H = a(M_p/3M_*)^{1/3}$ is the Hill radius for the planet of mass M_p (e.g., Liu et al. 2019). We assume a reference value of $W = 5.5R_H$ to compute M_p . The planet mass error bars are determined by solving for the maximum and minimum values of M_p via the gap width parameters $w_{\max} = 4.5$ and $w_{\min} = 7$, respectively. For several of the objects from the Long et al. (2018) sample, e.g., HL TAU and CI TAU, we instead rely on the results of published dedicated hydrodynamical simulations (Dipierro et al. 2015; Clarke et al. 2018). Zhang et al. (2018) lists DSHARP planet masses derived from detailed hydrodynamical simulations, including error bars. From their Table 3 we use only model $M_{p,am3}$ and DSD1 dust model, and omit the lower part of their table since most of the estimated masses there are consistent with 0 within the errors. For additional sources from other publications, TW Hya (Mentiply et al. 2019), GY 91 (Sheehan & Eisner 2018), HD 169142 (Pohl et al. 2017), PDS 70 (Keppler et al. 2019), we assume that the planet mass error is $\pm \log_{10}(2)$.

Fig. 1 shows the resulting planet mass histogram, the candidate planet mass versus separation, and mass versus age of the system. Our mass histogram (pale red with error bars) is rather similar to that derived by L19 (shown with the green colour).

3 POPULATION SYNTHESIS MODELING

In brief, to compare theoretical predictions to observations, we accept a simplified model for the protoplanetary disc structure and evolution. A massive core is then injected into the disc and allowed to grow and undergo the runaway gas accretion growth at rate $C^{-1}\dot{M}_{ra}$, where $C \geq 1$ is a dimensionless factor, and \dot{M}_{ra} is the runaway rate given by one of three runaway models from the literature described below. The population synthesis is terminated at the age of the ALMA systems and the resulting planet masses are compared to those of the candidate ALMA planets. A reasonable agreement is found for $C \sim 10$.

We model the disc surface density as a power law in radius with a time dependent normalization,

$$\Sigma(R, t) = \frac{M_d(t)}{2\pi R(R_{out} - R_{in})}, \quad (1)$$

where M_d is the disc mass between radii $R_{in} = 5$ AU and $R_{out} = 100$ AU. The disc mass is evolved according to

$$\frac{dM_d}{dt} = -\frac{M_d}{t_{disp}} - \dot{M}_g, \quad (2)$$

where \dot{M}_g is the gas accretion rate onto the planet, and the disc dispersal time is $t_{disp} = 2$ Myr. The initial disk mass is a uniform random variable with the minimum and maximum disc masses of $0.025M_\odot$ and $0.1M_\odot$, respectively, whereas stellar mass is $M_* = 1M_\odot$. The disc is in a vertical hydrostatic equilibrium, i.e. the geometric aspect ratio is $H/R = \sqrt{k_b T R / (G M_* \mu)}$, where k_b is the Boltzmann's constant, G is the gravitational constant, $\mu = 2.45m_p$ is the mean molecular weight where m_p is the proton mass, and the disc midplane temperature T is given by $T = T_0(R_0/R)^{1/2}$ where $T_0 = 20$ K and $R_0 = 100$ AU. We fix the disc α -viscosity parameter (Shakura & Sunyaev 1973) at $\alpha = 0.005$. The value of α affects the disc gap opening condition, for which we follow Crida et al. (2006) results, and may also affect gas accretion rates onto the planets depending on the exact scenario described below.

A growing core is injected into the disc at separation R , where R is a random variable with a uniform distribution in the $\log R$ space between $R = 10$ AU and $R = 140$ AU. We neglect planet migration for clarity of the argument. The classical runaway accretion phase duration is as short as $\sim 10^4$ years (D'Angelo et al. 2003), implying that the orbital separation of the planet will shrink by a small fraction only during the runaway phase. For example, Dipierro et al. (2018) model the rings and gaps in the dusty disc of Elias 24 (one of the systems included in our paper). Their planet grows from mass of $0.15M_J$ to $0.7M_J$ in about 4.4×10^4 years, during which it migrates from 65 AU to 61.7 AU only. Population synthesis with the three widely known models also shows that planets born beyond tens of AU do not start to migrate appreciably until the mass of $1 - 3M_J$ (e.g., see Fig.

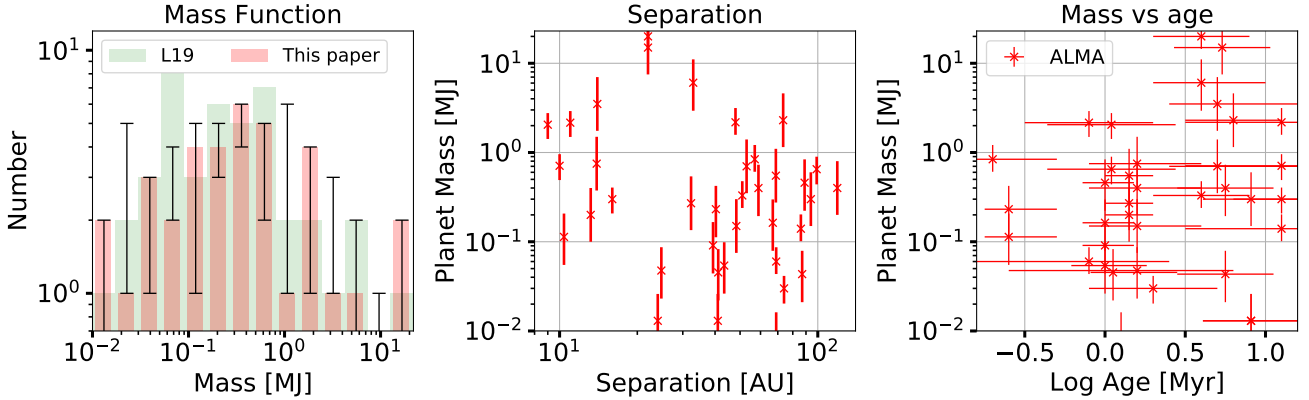


Figure 1. Data from Table A. **Left:** The candidate planet mass histogram from Table A, shown with the red color and the error bars. The green histogram shows the planet masses from L19 for comparison; **Middle:** Mass versus separation; **Right:** Planet mass versus age of the system.

3 in Ida et al. 2018), which is more massive than most of the ALMA planets.

We tested two methods of injecting massive solid cores into the disc and obtained very similar results. In the first, the cores are injected into the disc with mass large enough (e.g., 10–20 M_{\oplus}) for the runaway accretion to start immediately, and the core injection time, t_0 , was a random variable distributed uniformly in the log space between 0.1 Myr and 1 Myr. In the second method, presented in the paper, the cores are injected in the disc at time $t_0 = 0$ with smaller initial mass, $M_c = 1 M_{\oplus}$. The cores then accrete solids at a rate, \dot{M}_c , that is a uniform random variable in the log space in the limits between $3 \times 10^{-6} M_{\oplus} \text{ yr}^{-1}$ and $3 \times 10^{-5} M_{\oplus} \text{ yr}^{-1}$. We found that choosing larger values of \dot{M}_c does not affect our conclusions on C but reduces the number of sub-critical cores which have not yet entered the runaway valley. Choosing $\dot{M}_c \ll 3 \times 10^{-6} M_{\oplus} \text{ yr}^{-1}$ leads to too few massive cores $M_c \gtrsim 10 M_{\oplus}$, and hence too few gas giants, failing to explain the data.

The gas envelope of the planet grows at the rate

$$\dot{M}_g = \frac{M_p}{t_{\text{kh}}}, \quad (3)$$

where t_{kh} is the Kelvin-Helmholtz timescale of the envelope (Ikoma et al. 2000; Ida & Lin 2004a), which we write as

$$t_{\text{kh}} = 10^3 \text{ yr} \left(\frac{100 M_{\oplus}}{M_p} \right)^3 \kappa_0, \quad (4)$$

where κ_0 is gas dust opacity in units of $1 \text{ cm}^2 \text{ g}^{-1}$ (see eq. 10 in Ida et al. 2018, we set $\kappa_0 = 1$ in this paper except for the Bern model). The total accretion rate of solids and gas is the sum $\dot{M}_p = \dot{M}_c + \dot{M}_g$. We terminate accretion of solids when $M_p \geq 30 M_{\oplus}$ ¹. The above model for planetary growth is capped by the disc-limited runaway gas accretion rate \dot{M}_{ra} that is different for the three population synthesis scenarios explored below:

¹ Gas accretion dominates strongly at these masses anyway, but also ALMA observations show that the total disc dust masses are $\sim 30 - 100 M_{\oplus}$ (Long et al. 2018; Dullemond et al. 2018).

- In the IL04 model (Ida & Lin 2004a,b), the runaway accretion rate is given by $\dot{M}_{\text{ra}} = \dot{M}_d \exp(-M_p/M_{\text{th}})$, where $\dot{M}_d = 3\pi\alpha c_s H \Sigma$ is the unperturbed viscous disc accretion rate, and the thermal mass $M_{\text{th}} = 120 M_{\oplus} (R/\text{AU})^{3/4}$ takes into account gap opening that assumes to terminate gas supply to the planet.

- In the Bern model (Mordasini et al. 2012b), the gas runaway accretion rate depends on whether the planet opened a deep gap in the disc or not. In the former case, $\dot{M}_d = 3\pi\alpha c_s H \Sigma$. In the latter case, $\dot{M}_{\text{ra}} = \Sigma \Omega R_{\text{gc}}^3 H^{-1}$, where R_{gc} is the gas capture radius (their eq. 14). We employ the Crida et al. (2006) gap opening condition to select the appropriate limit. Following the authors, we use a reduced dust opacity $\kappa_0 = 0.003$.

- In the Tanigawa & Tanaka (2016) (TT16 hereafter), the runaway gas accretion rate is the minimum of two expressions. The first, gas accretion in the embedded phase, is given by $\dot{M}_{\text{emb}} = 0.29 (M_p/M_*)^{2/3} R^4 \Omega \Sigma_{\text{pert}} H^{-2}$, where $\Sigma_{\text{pert}} = \Sigma(R, t) / (1 + 0.034K)$ is the disc surface density perturbed by the presence of the planet, with the factor given by $K = (R/H)^5 (M_p/M_*)^2 \alpha^{-1}$. The second is the maximum of the global viscous disc accretion rate, \dot{M}_d , specified previously, and the "local" rate (eq. 13 in Tanigawa & Tanaka 2016) that is applicable only while the planet is clearing its local gas reserves. We neglect the latter phase for simplicity and note that its inclusion would require an even larger accretion rate suppression.

Finally, we apply the suppression factor $C \geq 1$ for all the models and compare the three models with observation. We do not allow the planets to exceed the mass of 10 M_J in order to remain in the planetary regime.

4 COMPARISON OF RESULTS TO OBSERVATIONS

L19 used population synthesis and asked how the ALMA planet candidates will evolve by the time their discs are dispersed. Here we ask a complementary question: can we form the observed population of ALMA planets within the widely accepted framework for planetary growth? Therefore, we terminate our population synthesis at the age of the ALMA

discs. In practice, the termination time of our models is randomly selected from the list of the stellar ages (shown in Table A), t_A , multiplied by a random number between 0.5 and 1.5. This multiplication bears no practical importance but improves visibility of population synthesis planet ages in the figures.

Fig. 2 compares the mass function of ALMA planets, shown with the gray histogram, with the resulting mass distribution of the three population synthesis calculations for various values of C . The nominal runaway gas accretion models (red, $C = 1$) are inconsistent with the data. The Bern model shows the smallest disagreement since its nominal accretion rate \dot{M}_{ra} is lower than the two other models. In all cases there is a synthetic planet desert between the mass of $\sim 0.1 M_J$ to several M_J . The population of very massive gas giants seen in the synthetic models should be easily observable in the ALMA data as such planets open gaps not only in dust but also in gas, but such planets are rare. Suppression of gas accretion rates by factors of $C > 1$ reduces the disagreement between the models and the data. Qualitatively, the models with $C = 15, 5$ and 20 , for the IL04, Bern and TT16 models, respectively, produce reasonable planet mass functions (solid green curves).

Fig. 3 shows the synthetic planet masses versus system ages for two of the models ($C = 5$ Bern and $C = 20$ TT16 models), compared to ALMA data (red symbols with the error bars). The synthetic planets show a trend of increasing planet mass with the system age, which is to be expected. Synthetic planets more massive than $1 M_J$ are usually older than ~ 3 Myrs. It is not clear if the current ALMA data support or challenge theoretical predictions. There are several massive planets too young for their masses for the population models to reproduce, however the age estimates have significant uncertainties.

5 DISCUSSION AND CONCLUSIONS

We showed that the runaway gas accretion scenario predicts too few sub-Jupiter mass giants and too many $\gtrsim 3 M_J$ planets compared with the candidate ALMA planets. Reduction in the efficiency of gas accretion by a factor of order 10 results in a better agreement of theory and observations.

Although icelines, dead zone transition, secular gravitational instability and other effects were proposed to explain the observed ringed dust structures *instead of* planets (Zhang et al. 2015; Pinilla et al. 2016; Flock et al. 2015; Takahashi & Inutsuka 2014), these are not likely to account for most of the observations because there is no correlation between the structures and thermal disc properties, and because some of the rings are narrower than the disc scale-height H (Long et al. 2018; Huang et al. 2018; Zhang et al. 2018).

Some authors suggested that candidate planets are less massive than the typically inferred \sim Saturn masses, e.g., $\sim 10 - 20 M_{\oplus}$ in Boley (2017); $M_p \sim 1 - 60 M_{\oplus}$ in Dong et al. (2018). However, planets less massive than $\sim 10 M_{\oplus}$ are unlikely to work for most sources as the disc viscosity parameter required in these scenarios, $\alpha \lesssim 10^{-4}$, is too small to account for the observed ring profiles (see §5.3 in Dullemond et al. 2018), and also cannot explain the observed stellar accretion rates, assuming a viscous angular momentum

transport in the disc (see Clarke et al. 2018). Furthermore, runaway gas accretion sets in at lower core masses – as low as $\sim 5 M_{\oplus}$ at wide separations (Piso & Youdin 2014). Therefore, the exact planet masses are not crucial for validity of our argument as long as the planets are more massive than $\sim 10 M_{\oplus}$; the runaway gas accretion would still happen and the results would then diverge from the ALMA observations significantly. There are also suggestions that planets may be larger, e.g., $M_p \sim 1 M_J$ (Bae et al. 2018). However, $M_p \sim 1 M_J$ planets are inside the “forbidden” middle region of the runaway valley. The mere (wide-spread) existence of such planets at large separations would again challenge an unabated runaway growth scenario. On the other hand, the number of planets in ALMA discs may be smaller since planets may open more than one gap for low disc viscosities (Dong et al. 2018).

Based on observations of planets at separations less than a few AU, gas giant planets were suggested to not grow via the Core Accretion scenario beyond the gap-opening mass (e.g., Ida & Lin 2004a,b; Santos et al. 2017; Suzuki et al. 2018). Our results extend these suggestions in several ways. Firstly, ALMA planet candidates are separated by $\sim 10 - 100$ AU from their host stars. Further, their gaseous discs are not yet dispersed, so yield “live” constraints on the process of planet accretion. Finally, most of the planet candidates are not massive enough to open significant gaps in the gas (Dipierro et al. 2015; Clarke et al. 2018; Dipierro & Laibe 2017), so their low gas accretion rates cannot be explained by gap opening.

One reason for the inefficiency of gas accretion may be dust opacity. To obtain the envelope contraction time scales within a few Myr, dust opacity is typically assumed to be $\sim 10 - 100$ times lower than the interstellar dust opacity due to dust growth (Pollack et al. 1996; Papaloizou & Nelson 2005; Lissauer et al. 2009; Ayliffe & Bate 2012; Piso et al. 2015). However, dust growth could be counteracted by grain fragmentation (Dullemond & Dominik 2005; Helled & Bodenheimer 2011; Mordasini 2013), an effect that increases the opacity. Further, composition of gas envelopes of giant planets may be strongly over-abundant in metals and dust for two reasons: (i) the bulk composition of planets is significantly over-abundant in metals compared to their parent stars (Miller & Fortney 2011); and (ii) gas giant planets tend to be found preferentially around metal-rich stars (Fischer & Valenti 2005). These two effects may increase envelope dust opacity by a factor of a few to ten compared with that of the interstellar medium at Solar metallicity. Ayliffe & Bate (2009a) finds that gas accretion rate onto a $10 - 50 M_{\oplus}$ core is at least an order of magnitude lower for the full interstellar dust opacity case compared with that for opacity reduced by a factor of 100.

Additionally, classic hydrostatic calculations of envelope contraction (e.g., Ikoma et al. 2000) assumed 1D geometry. Modern 3D simulations (Szulágyi et al. 2014; Ormel et al. 2015; Fung & Chiang 2016; Lambrechts & Lega 2017) show that there is not only an inflow but also an outflow from the Hill sphere of the planet. This outflow is part of the meridional circulation between the circumstellar and circumplanetary discs in the case of giant planets (Szulágyi et al. 2014; Fung & Chiang 2016). In the terrestrial regime, a similar recycling of gas within the Bondi-radius has been found (Ormel et al. 2015). In both planetary mass regimes,

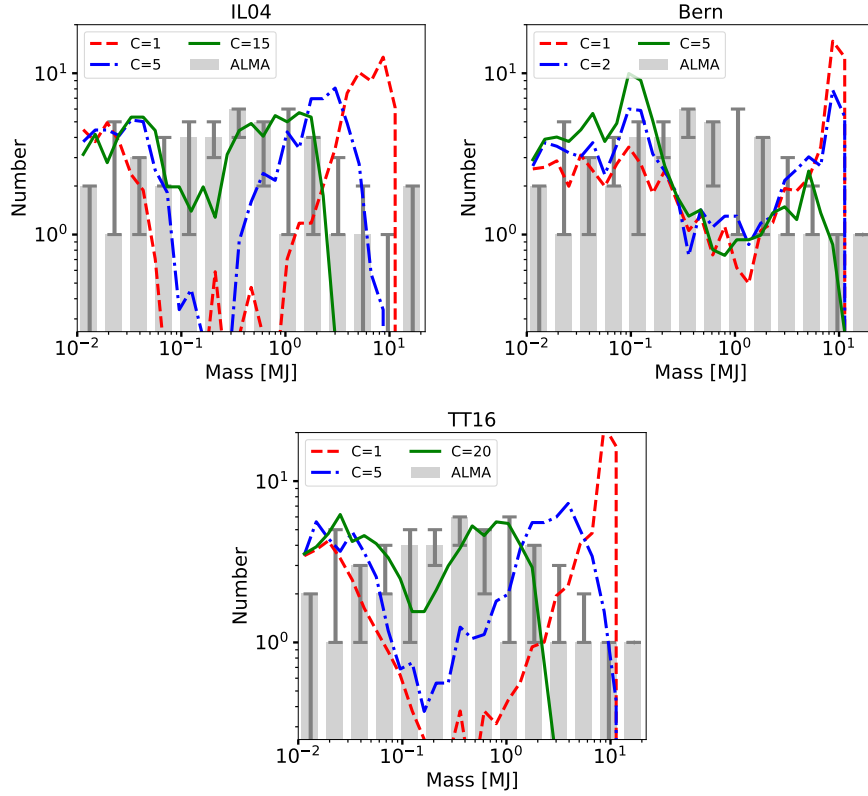


Figure 2. The mass function for the three population synthesis models (colored curves) of runaway accretion growth compared to ALMA observations (gray). The normalization of synthetic planet populations was scaled down to match the total number of ALMA planets. Gray capped vertical lines shows estimated observational errors. Note that all of the models over-predict the population of massive gas giant planets strongly for $C = 1$. The gas runaway accretion rate needs to be suppressed by the factor of $\sim 5 - 25$ to yield a reasonable match to the observed mass function.

the gas flow enters the Hill sphere from the vertical directions and leaves through the midplane region, leading to a reduction in the gas accretion rate.

ACKNOWLEDGEMENTS

SN acknowledges support from STFC grants ST/N000757/1 and ST/M006948/1 to the University of Leicester. G.D. acknowledges financial support from the European Research Council (ERC) under the European Union’s Horizon 2020 research and innovation programme (grant agreement No 681601). J.Sz. acknowledges the funding from the the Swiss National Science Foundation (SNSF) Ambizione grant PZ00P2_174115.

REFERENCES

ALMA Partnership et al., 2015, *ApJ*, 808, L3
 Adibekyan V., 2019, arXiv e-prints,
 Andrews S. M., et al., 2018, *ApJ*, 869, L41
 Ayliffe B. A., Bate M. R., 2009a, *MNRAS*, 393, 49
 Ayliffe B. A., Bate M. R., 2009b, *MNRAS*, 397, 657
 Ayliffe B. A., Bate M. R., 2012, *MNRAS*, 427, 2597
 Bae J., Pinilla P., Birnstiel T., 2018, *ApJ*, 864, L26
 Bate M. R., Bonnell I. A., Bromm V., 2003, *MNRAS*, 339, 577
 Boley A. C., 2017, *ApJ*, 850, 103

Cimerman N. P., Kuiper R., Ormel C. W., 2017, *MNRAS*, 471, 4662
 Clarke C. J., et al., 2018, *ApJ*, 866, L6
 Crida A., Morbidelli A., Masset F., 2006, *Icarus*, 181, 587
 D’Angelo G., Henning T., Kley W., 2003, *ApJ*, 599, 548
 Dipierro G., Laibe G., 2017, *MNRAS*, 469, 1932
 Dipierro G., Price D., Laibe G., Hirsh K., Cerioli A., Lodato G., 2015, *MNRAS*, 453, L73
 Dipierro G., et al., 2018, *MNRAS*, 475, 5296
 Dong R., Li S., Chiang E., Li H., 2018, *ApJ*, 866, 110
 Dullemond C. P., Dominik C., 2005, *A&A*, 434, 971
 Dullemond C. P., et al., 2018, *ApJ*, 869, L46
 Fischer D. A., Valenti J., 2005, *ApJ*, 622, 1102
 Flock M., Ruge J. P., Dzyurkevich N., Henning T., Klahr H., Wolf S., 2015, *A&A*, 574, A68
 Fung J., Chiang E., 2016, *ApJ*, 832, 105
 Goda S., Matsuo T., 2019, *ApJ*, 876, 23
 Haisch Jr. K. E., Lada E. A., Lada C. J., 2001, *ApJ*, 553, L153
 Helled R., Bodenheimer P., 2011, *Icarus*, 211, 939
 Huang J., et al., 2018, *ApJ*, 869, L42
 Ida S., Lin D. N. C., 2004a, *ApJ*, 604, 388
 Ida S., Lin D. N. C., 2004b, *ApJ*, 616, 567
 Ida S., Tanaka H., Johansen A., Kanagawa K. D., Tanigawa T., 2018, *ApJ*, 864, 77
 Ikoma M., Nakazawa K., Emori H., 2000, *ApJ*, 537, 1013
 Keppler M., et al., 2019, arXiv e-prints,
 Lambrechts M., Lega E., 2017, *A&A*, 606, A146
 Lee E. J., Chiang E., Ormel C. W., 2014, *ApJ*, 797, 95
 Lissauer J. J., Hubickyj O., D’Angelo G., Bodenheimer P., 2009, *Icarus*, 199, 338

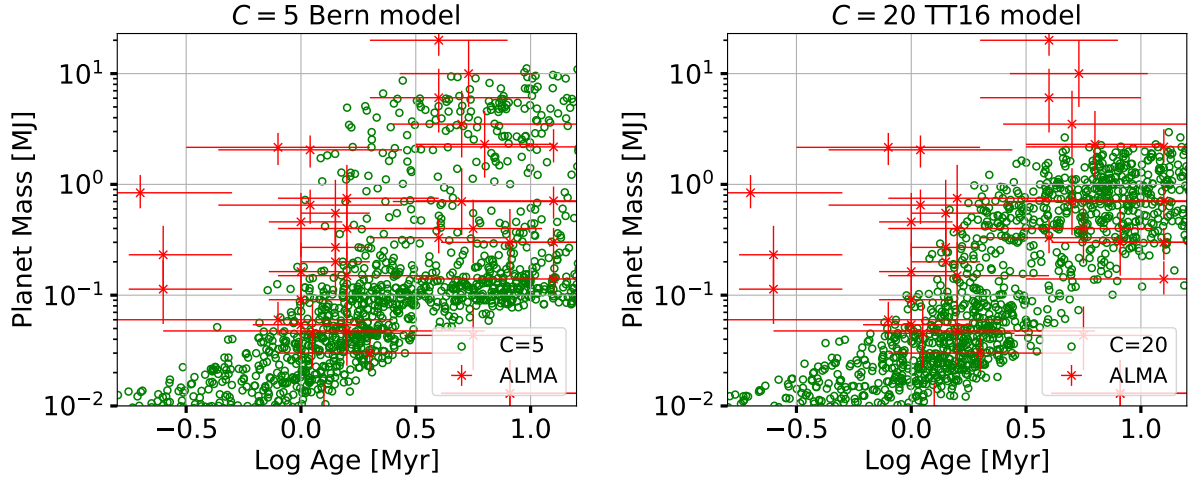


Figure 3. Distribution of the ALMA data in the planet mass versus stellar age compared to the two synthetic models with the reasonable values of C as indicated in the legends. This mass-age correlation that may be useful to test theoretical models against the data in the future.

Liu Y., et al., 2019, *A&A*, 622, A75
 Lodato G., et al., 2019, *MNRAS*, 486, 453
 Long F., et al., 2018, preprint, ([arXiv:1810.06044](https://arxiv.org/abs/1810.06044))
 Maldonado J., Villaver E., Eiroa C., Micela G., 2019, arXiv e-prints,
 Mayor M., et al., 2011, ArXiv e-prints (astro-ph 1109.2497),
 Mentiplay D., Price D. J., Pinte C., 2019, *MNRAS*, 484, L130
 Miller N., Fortney J. J., 2011, *ApJ*, 736, L29
 Mizuno H., Nakazawa K., Hayashi C., 1978, *Progress of Theoretical Physics*, 60, 699
 Mordasini C., 2013, *A&A*, 558, A113
 Mordasini C., Alibert Y., Benz W., Naef D., 2009, *A&A*, 501, 1161
 Mordasini C., Alibert Y., Benz W., Klahr H., Henning T., 2012a, *A&A*, 541, A97
 Mordasini C., Alibert Y., Klahr H., Henning T., 2012b, *A&A*, 547, A111
 Ormel C. W., Shi J.-M., Kuiper R., 2015, *MNRAS*, 447, 3512
 Papaloizou J. C. B., Nelson R. P., 2005, *A&A*, 433, 247
 Pinilla P., Flock M., Ovelar M. d. J., Birnstiel T., 2016, *A&A*, 596, A81
 Piso A.-M. A., Youdin A. N., 2014, *ApJ*, 786, 21
 Piso A.-M. A., Youdin A. N., Murray-Clay R. A., 2015, *ApJ*, 800, 82
 Pohl A., et al., 2017, *ApJ*, 850, 52
 Pollack J. B., Hubickyj O., Bodenheimer P., Lissauer J. J., Podolak M., Greenzweig Y., 1996, *Icarus*, 124, 62
 Safronov V. S., 1972, *Evolution of the protoplanetary cloud and formation of the earth and planets.* Jerusalem (Israel): Israel Program for Scientific Translations, Keter Publishing House, 212 p.
 Santos N. C., et al., 2017, preprint, ([arXiv:1705.06090](https://arxiv.org/abs/1705.06090))
 Schlaufman K. C., 2018, *ApJ*, 853, 37
 Shakura N. I., Sunyaev R. A., 1973, *A&A*, 24, 337
 Sheehan P. D., Eisner J. A., 2018, *ApJ*, 857, 18
 Suzuki D., et al., 2016, *ApJ*, 833, 145
 Suzuki D., et al., 2018, *ApJ*, 869, L34
 Szulágyi J., 2017, *ApJ*, 842, 103
 Szulágyi J., Mordasini C., 2017, *MNRAS*, 465, L64
 Szulágyi J., Morbidelli A., Crida A., Masset F., 2014, *ApJ*, 782, 65
 Szulágyi J., Masset F., Lega E., Crida A., Morbidelli A., Guillot T., 2016, *MNRAS*, 460, 2853

Takahashi S. Z., Inutsuka S.-i., 2014, *ApJ*, 794, 55
 Tanigawa T., Tanaka H., 2016, *ApJ*, 823, 48
 Troup N. W., et al., 2016, *AJ*, 151, 85
 Zhang K., Blake G. A., Bergin E. A., 2015, *ApJ*, 806, L7
 Zhang S., et al., 2018, *ApJ*, 869, L47

APPENDIX A: DATA TABLE

This paper has been typeset from a $\text{\TeX}/\text{\LaTeX}$ file prepared by the author.

Source	Age [Myr]	Sep [AU]	Planet mass [M_J]
RY TAU	1.00	43.41	0.054
UZ TAUE	1.26	69.00	0.009
DS TAU	3.98	32.93	6.058
FT TAU	1.58	24.78	0.048
MWC 480	6.31	73.43	2.300
DN TAU	2.51	49.29	0.005
GO TAU	5.62	58.91	0.399
GO TAU	5.62	86.99	0.043
IQ TAU	1.12	41.15	0.045
DL TAU	1.00	39.29	0.091
DL TAU	1.00	66.95	0.163
DL TAU	1.00	88.90	0.459
CI TAU	1.58	13.92	0.750
CI TAU	1.58	48.36	0.150
CI TAU	1.58	118.99	0.400
HL TAU	1.41	13.20	0.200
HL TAU	1.41	32.30	0.270
HL TAU	1.41	68.80	0.550
AS 209	1.10	9.00	2.050
AS 209	1.10	99.00	0.650
EL 24	0.20	57.00	0.840
EL 27	0.79	69.00	0.060
GW Lup	2.00	74.00	0.030
HD 142666	12.59	16.00	0.300
HD 143006	3.98	22.00	20.000
HD 143006	3.98	51.00	0.330
HD 163296	12.59	10.00	0.710
HD 163296	12.59	48.00	2.180
HD 163296	12.59	86.00	0.140
SR 4	0.79	11.00	2.160
GY 91	0.25	10.40	0.113
GY 91	0.25	40.30	0.232
GY 91	0.25	68.90	0.002
TW Hya	8.13	24.00	0.013
TW Hya	8.13	41.00	0.013
TW Hya	8.13	94.00	0.300
HD 169142	5.01	14.00	3.500
HD 169142	5.01	53.00	0.700
PDS 70	5.37	22.00	15.000

Table A1. The data used in this paper. The columns indicate, respectively: (1) star name; (2) age ; (3) gap location; (4) inferred planet mass. See Section 2 for references and error determination.